Research Article | Vol. 29, No. 7 / 29 March 2021 / Optics Express 10140
Optics EXPRESS

Low noise 400 W coherently combined single frequency laser beam for next generation gravitational wave detectors

FELIX WELLMANN,[1,2,5,6] NINA BODE,[2,3,5,7] PETER WESSELS,[1,2] LUDGER OVERMEYER,[1,2,4] JÖRG NEUMANN,[1] BENNO WILLKE,[2,3] AND DIETMAR KRACHT[1,2]

[1]*Laser Zentrum Hannover e.V., Hollerithallee 8, 30419 Hannover, Germany*
[2]*Cluster of Excellence QuantumFrontiers, Welfengarten 1, 30167 Hannover, Germany*
[3]*Max-Planck-Institut für Gravitationsphysik (Albert-Einstein-Institut) and Institut für Gravitationsphysik, Leibniz Universität Hannover, Callinstr. 38, 30167 Hannover, Germany*
[4]*Institut für Transport- und Automatisierungstechnik, Leibniz Universität Hannover, An der Universität 2, 30823 Garbsen, Germany*
[5]*Authors contributed equally*
[6]*f.wellmann@lzh.de*
[7]*nina.bode@aei.mpg.de*

Abstract: Design studies for the next generation of interferometric gravitational wave detectors propose the use of low-noise single-frequency high power laser sources at 1064 nm. Fiber amplifiers are a promising design option because of their high output power and excellent optical beam properties. We performed filled-aperture coherent beam combining with independently amplified beams from two low-noise high-power single-frequency fiber amplifiers to further scale the available optical power. An optical power of approximately 400 W with a combining efficiency of more than 93% was achieved. The combined beam contained 370 W of linearly polarized TEM_{00}-mode and was characterized with respect to the application requirements of low relative power noise, relative beam pointing noise, and frequency noise. The noise performance of the combined beam is comparable to the single amplifier noise. This represents, to our knowledge, the highest measured power in the TEM_{00}-mode of single frequency signals that fulfills the low noise requirements of gravitational wave detectors.

1. Introduction

The first direct observation of a gravitational wave by interferometric gravitational wave detectors (GWD) [1] in 2015 demonstrated a new method for studying the universe. Several further detections, partly confirmed by independent observations in the electromagnetic spectrum [2], led to multiple studies of a new generation of GWDs with significantly increased sensitivity. These design studies [3–5] propose GWD designs which will allow the detection of more distant and fainter astrophysical events and enable improved multi-messenger astronomy [2]. One design approach that drives the laser development at 1064 nm is the operation of the interferometer at room temperature with up to 500 W laser power [4]. Other detector studies propose longer wavelengths at e.g. 2 µm in combination with cryogenic cooled GWD test masses. As previously demonstrated, the 1064 nm laser systems could potentially be used to generate 2 µm light via degenerated optical parametric down-conversion [6].

The current generation of GWDs relies on crystal based lasers and amplifiers with an optical power of 100–200 W [7–9]. Fiber technology has been identified as an alternative to overcome power scaling limitations, while providing excellent beam quality and noise properties with low system complexity [10]. Fiber-based single-frequency amplifiers are primarily limited by

#420350 https://doi.org/10.1364/OE.420350
Journal © 2021 Received 20 Jan 2021; revised 5 Mar 2021; accepted 9 Mar 2021; published 16 Mar 2021

Optics EXPRESS

excessive power noise induced by stimulated Brillouin scattering (SBS) [11] or in some cases by transverse mode instabilities [12]. Laser output power scaling for the application of gravitational wave detection was investigated by the use of custom-made specialty fiber designs such as photonic-crystal-fibers [12–14], chirally-coupled-core fibers [15], and fibers with strongly doped cores and low numerical apertures [16]. However, potential drawbacks of these fibers can be: no availability because of patent protection, unknown reproducibility between fiber drawing batches, unproven reliability, and designs that are complex, difficult, and costly to reproduce. Furthermore, in some cases (e.g. PCF) a monolithic amplifier with integrated fiber components has not been demonstrated at the required power level.

An alternative approach is the use of commercially established standard step-index-fibers and coherently combine beams from several systems to reach the desired optical power while preserving low noise properties [17,18]. In most cases in the Yb-band, these fibers are well-known by the industry, are long-term tested, are available and show constant performance over multiple fiber drawing batches. Coherent beam combining (CBC) using a filled-aperture approach is primarily investigated for the use in GWDs, because of the required high TEM_{00}-mode content. Thus, tiled aperture combining [19,20] with overlapping beams in the far field is not usable. Published CBC systems with kHz linewidth demonstrated either very high output power levels (above 1 kW) with unknown (not published) beam properties or low power systems (below 100 W) with extensive verification of preserved beam properties. The current power record is held by Flores et al. [21] with more than 1 kW of output power by the use of three PCF-based and free-space pumped amplifiers. They demonstrated that power scaling up to the kilowatt level can be achieved via CBC. However, the noise properties and the TEM_{00}-mode content, which are essential parameters for the application of gravitational wave detection, remain unknown. Tünnermann et al. [17] demonstrated that the filled-aperture CBC preserves the beam quality by measuring the TEM_{00}-mode content and that CBC with no significant noise increase compared to the single amplifier performance is feasible. They combined two 10 W single-frequency beams and evaluated both the frequency and the relative power noise. Wei et al. [18] used two 40 W fiber amplifiers and extensively studied the noise properties; this includes relative power noise, frequency noise and relative beam pointing of the combined beams.

Similar to the work of Tünnermann et al. [17], we set up a Mach-Zehnder interferometer using a single low-noise seed source and placed two high power amplifier chains within the two arms of the CBC setup. The amplifier architecture and performance was previously reported [22,23] and is capable of producing more than 200 W of output power. The two amplified beams were coherently combined by controlling the phase of the interfering beams and the properties of the combined beam were characterized with respect to the requirements of gravitational wave detectors. This includes the evaluation of the TEM_{00}-mode content, the relative power noise, the relative pointing noise and the frequency noise.

2. Coherent beam combining setup and phase controller characteristics

Figure 1 shows the CBC system setup, comprised of a common seed laser, two pre-amplifiers, and two main-amplifier modules in a Mach-Zehnder arrangement. A non-planar ring oscillator (NPRO) with 2 W of output power, 1 kHz linewidth (measured over 100 ms), and low noise properties was split into two beam paths. The two beams from the NPRO were each independently amplified in two amplifier chains and are recombined at a 50/50 beam combining element. Both amplifier output beams were independently mode-matched to an optical ring resonator located within a beam diagnostic tool (diagnostic breadboard - DBB [24]). Thus, a sufficient spatial overlap of both beams in the near- and far field and therefore efficient beam combining was ensured. The DBB was further used to characterize the combined beam (see Chapter 3.). The stabilization of the relative phase between both interferometer arms was achieved using a standard heterodyne technique. One interferometer arm was equipped with an electro-optical-modulator to

Optics EXPRESS

generate 12 MHz phase modulated side-bands. These sidebands were used as the phase references in a heterodyne readout scheme to measure the relative phase between the two interfering light fields on the combining element. Therefore, a fraction of the interferometer output beam was detected with a photodiode. The signal of this photodiode was demodulated at 12 MHz to produce an error signal for the feedback control used to adjust the phase of the interfering beams for constructive interference. The relative phase was stabilized using two actuators. The open loop transfer function of the control loop is shown in Fig. 2. As a low frequency phase actuator, a fiber stretcher (OPTIPHASE, PZ2-PM2) with approximately 40 m of fiber and a maximum optical path displacement of up to 2240 µm was placed in the low power path of one interferometer arm. This stretcher enables long-term stable locking performance and was used to stabilize phase variations up to approximately 25 Hz (see actuator signals in Fig. 8). The first resonance of the fiber stretcher is located at 18 kHz and must be suppressed because even though the fiber stretcher is only used for stabilizing low frequency phase variations, the large phase shift of more than 30 radV^{-1} could still lead to excessive current noise coupling into the phase control loop at high frequencies. This coupling was suppressed by using two low pass filters (cut-off

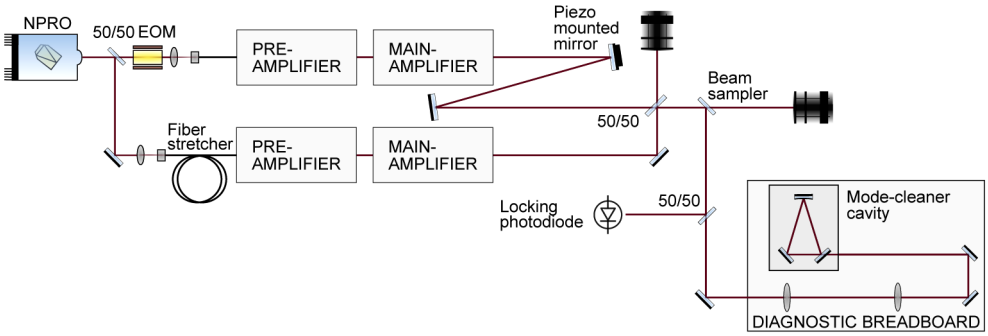

Fig. 1. CBC setup consisting of a common seed laser, two pre-amplifiers, and two main-amplifiers. Both amplified beams are superimposed at a 50/50 combining element and are aligned and mode-matched to the DBB's ring-cavity (mode-cleaner cavity). The relative phase is stabilized using a fiber stretcher and a piezo mounted mirror.

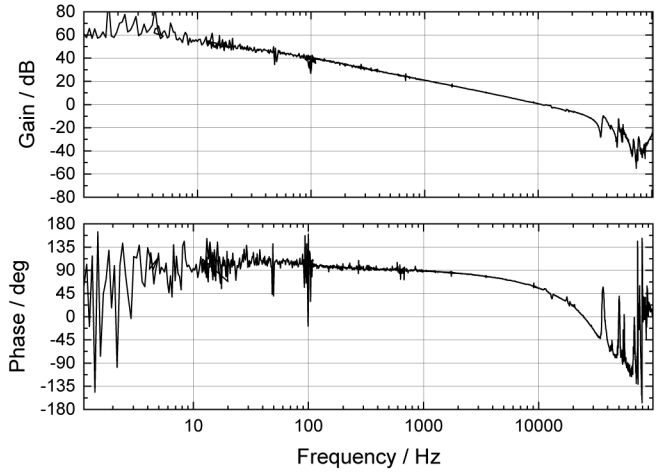

Fig. 2. Open loop transfer function with the unity gain frequency located at 10 kHz. Please note that the variation below 50 Hz is caused by limited averaging time.

Optics EXPRESS

frequencies located approximately at 25 Hz and 3 kHz) and a notch filter located at the resonance. Additionally, a mirror which was mounted on a piezoelectric transducer (PZT) (PI, P-010.05H) was used to stabilize variations up to 10 kHz (see actuator signals in Fig. 8) with a maximum actuator travel range of 10 µm. If a higher unity gain frequencies beyond 10 kHz should become necessary in future CBC experiments, using an EOM for high frequency phase shifting and concurrently generating the 12 MHz side-bands as done by Wei et al. [18] could be a viable option.

3. Optical performance

In this section, the optical properties of the combined beam in comparison with the beam of the single amplifiers is evaluated. The characterization was performed with respect to the application of gravitational wave detection. Therefore, the following was measured: combined power, combining efficiency, higher-order-mode (HOM) content and noise performance including relative power noise, frequency noise, and relative beam pointing noise. The DBB was used to evaluate the noise properties and the HOM content of the combined beam by the use of a free-space ring resonator. Furthermore, the differential phase noise between the CBC interferometer arms was evaluated by in-loop measurements of the phase control loop. The optical characteristics of the amplifiers were investigated and published in [23]. The amplifiers 2 and 4 from [23] were used for the CBC experiments. In accordance to the previously published paper the single amplifier noise performance is identically labeled within the following figures.

3.1. Combining efficiency and combined power

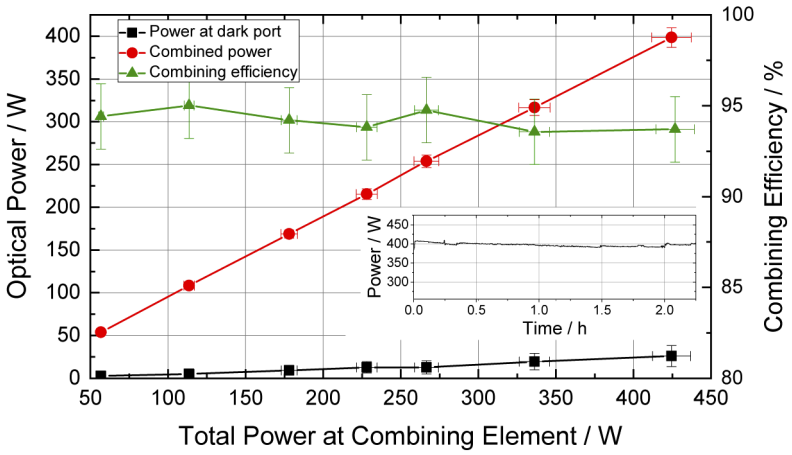

Fig. 3. Combined optical power, the loss at the dark port and the resulting combining efficiency over the total input power present at the combining element. Inset: Combined optical power over more than 2 h of operation.

Figure 3 shows the optical power of the combined beam, the power loss at the dark port and the combining efficiency at several power levels. The maximum combining efficiency is achieved with equal power at the input ports of the recombining beam splitter element and therefore the output power was set for one of the amplifiers and the other was adapted accordingly. The efficiency was measured to be around 93.8% at the combined output power of 398 W. The combining efficiency is affected by beam misalignment, mismode-matching, residual unequal laser power at the combining element, and HOMs with different phase relations. Stable operation was achieved at all power levels such that a detailed characterization of the combined beam was

Optics EXPRESS

possible. At approximately 400 W optical power 2 h of stable operation was demonstrated. The power variation during this period was less than 2% (RMS).

3.2. Beam quality

Gravitational wave detectors rely on the interference of the fundamental transverse mode that is injected into their interferometers. Other modes are removed by the use of mode-cleaner cavities. Thus, the laser system must provide a beam that consists primarily of the TEM_{00}-mode. The HOM-content of the amplifiers and of the combined beam was analyzed at several combined power levels and the TEM_{00}-mode content was calculated based on the mode-scan performed by the DBB. The HOM-content values are shown in Fig. 4. It can be seen, that the HOM-content increased with the individual amplifier output power and with the power in the combined beam. The reasons for increased HOM-content of the single amplifier is most probably related to saturation effects and thermal load caused by pumping the gain fiber. Although the HOM-content of the combined beam shows slightly degraded beam quality at some power levels, the beam quality at the highest combined power deviates less than 1% in HOM-content from that of the single amplifiers. The reasons for slightly increased HOM-content of the combined beam compared to the single amplifiers could be related to residual mismode-matching to the DBB's ring cavity, a deformed beam which can be the result of alignment error of the two beams, or thermal lensing within optical components such as the beam splitting element (Newport 10Q20HBS.33P) [25] placed in the beam path. It should be noted that the measured HOM-content of 6.9% is, to our knowledge, the lowest of single-frequency signals with a linewidth of 1 kHz at the power level of approx. 400 W. At this output power, the combined beam consisted of approximately 370 W in a linear polarized TEM_{00}-mode.

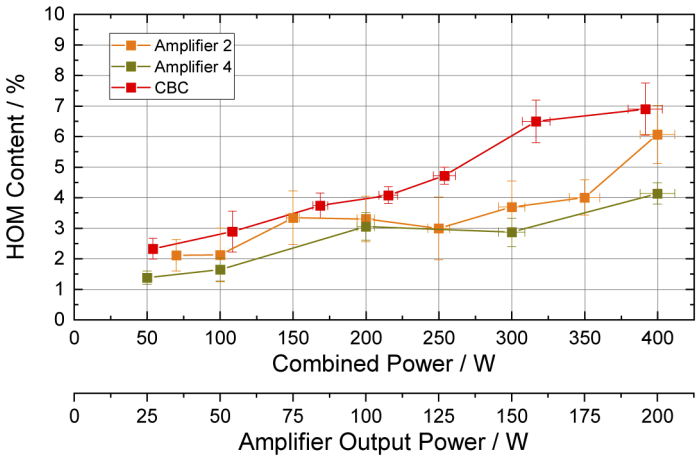

Fig. 4. HOM-content of the single amplifiers and the combined beam at several output powers of the single amplifiers and the combined beam.

3.3. Relative power noise

The relative power noise of the individual amplifiers and the combined beam was measured in the frequency band from 1 Hz to 100 kHz and is shown in Fig. 5. In general, pump power noise dominates the amplifier output power noise up to several kilohertz, while the seed laser power noise dominates at higher frequencies [26]. Despite this behavior and the strong attenuation of pump power noise at high frequencies, the pump noise can still affect the output power noise at high frequencies. Figure 5 shows slightly different power spectral densities for the

Optics EXPRESS

power noise of the two amplifiers, which are likely caused by different pump power noise performance. Furthermore, Fig. 5 shows the relative power noise of the combined laser beam, which is comparable to the power noise of the single amplifiers. It should be noted that the used optical components and the measurement setup was slightly different for each amplifier. The different component resonances and external perturbations can not be excluded as the reason for performance variations. Furthermore, in Fig. 5, amplifier 4 showed an irregularly occurring feature in the measurement at around 1kHz, which was likely of external origin. Although the relative power noise spectra showed some irregularities, the noise was dominated by the noise of the individual amplifiers. Overall, the noise performance of the amplifiers and the combined beam is comparable to currently used free-running laser systems [7,8].

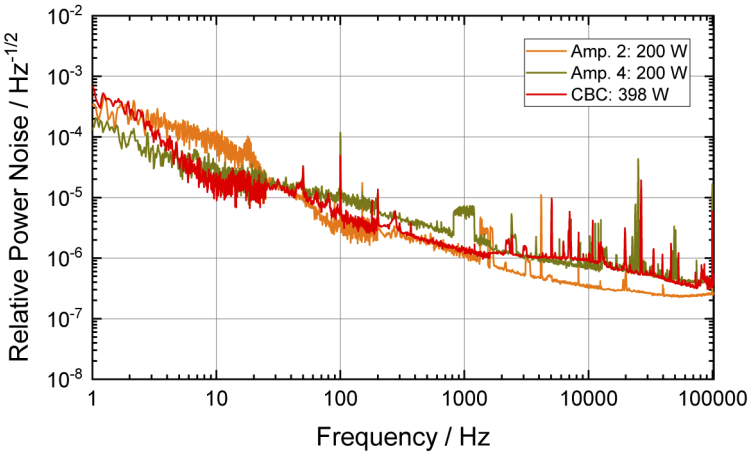

Fig. 5. Relative power noise of the combined beam in comparison with the single amplifier performance. Relative power noise variations are caused by the amplifier pumps.

It should be noted, that the application of gravitational wave detection requires much lower power noise which could be achieved by power stabilization systems that feed back to the seed power or the pump power of the amplifiers [7]. In the case that a CBC laser setup is used, the slow power drifts must be compensated by adjusting the output power of each amplifier to avoid contrast reduction of the CBC interferometer.

3.4. Relative beam pointing noise

Beam pointing (cf. [24] for the used definition of relative pointing noise) stability is crucial for the application of gravitational wave detection. Although the mode-cleaner cavity (cf. Section 3.2) will reduce the beam jitter on its transmitted beam, it will introduce a coupling of amplifier output beam jitter to power noise which must be actively stabilized. Residual beam pointing behind the mode-cleaner cavity can still affect the interferometer's sensitivity [27]. Thus, beam pointing noise of the high power laser before mode filtering must be sufficiently low (a noise comparison before and behind the mode-cleaner cavity and requirements can be found in e.g. [28]). The relative beam pointing noise of the combined beam was measured and is compared in Fig. 6 with the noise performance of amplifiers 2 and 4. Figure 6 shows that the noise level of the combined beam slightly increased in comparison with the single amplifier beam pointing. Several reasons, which include environmental variations such as mechanical motion and acoustic noise, could have affected the beam pointing noise. Furthermore, residual misalignment between the two beams at the beam splitting element and thus not perfectly collinear beams could have caused the observed variations of the beam pointing noise. The origin of the increased pointing could not be conclusively identified. Overall, the pointing noise of the combined high power

Optics EXPRESS

beam is in line with current pointing noise requirements of GWDs and is comparable to currently used laser systems [7,8].

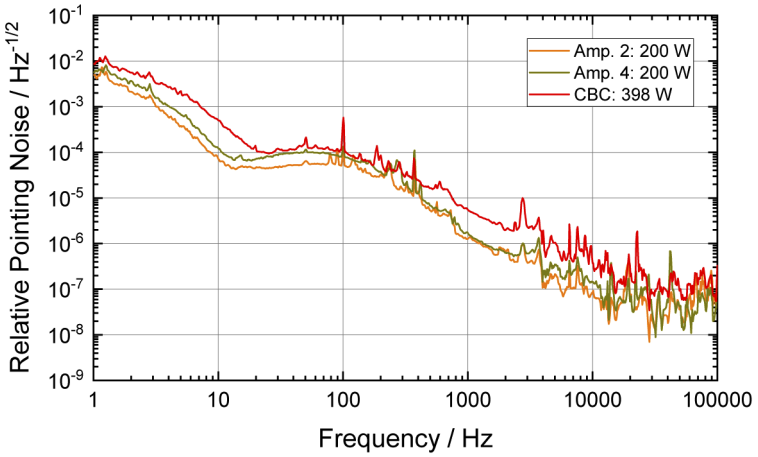

Fig. 6. Relative pointing noise spectrum of the amplifiers in comparison with the combined beam pointing noise.

3.5. *Frequency and differential phase noise*

The frequency noise of the combined beam was evaluated and compared to the measurements of the individual amplifiers to investigate potential additional noise contributions by CBC. As mentioned above, a seed signal with a linewidth of 1 kHz, integrated over 100 ms, was injected into both amplifier chains. In addition to phase noise caused by the amplifiers [29], environmental noise such as acoustic noise or thermal variations cause phase noise and, therefore, frequency noise. The measurement of the frequency noise of the combined beam, shown in Fig. 7, did not show additional noise features compared to the individual amplifiers within the frequency range of 1 Hz–100 kHz. It should be noted that the peak at approximately 8 kHz was caused by the

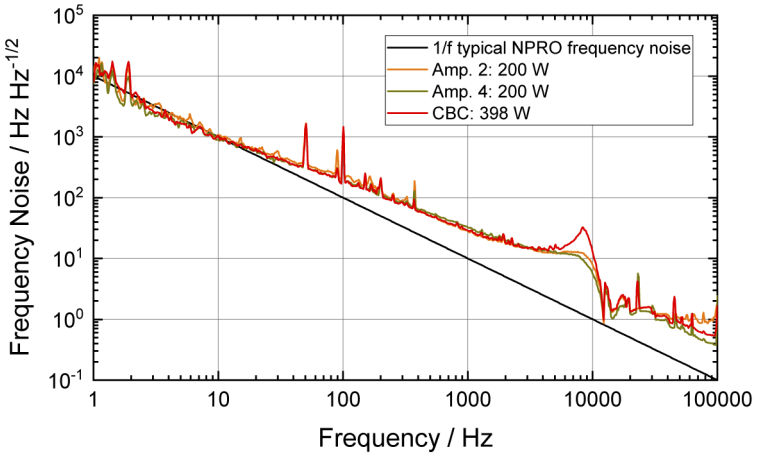

Fig. 7. Frequency noise measurements of the amplifiers and the combined beam show comparable noise performance. Note that the feature at around 8 kHz was caused by the measurement setup.

Optics EXPRESS

locking electronics of the DBB. The measurements shown in Fig. 7 indicate, that the frequency noise is dominated by the individual frequency noise of the amplifiers and seed source and not by the CBC. As the application requires lower frequency noise an active stabilization must be applied [28], which would be neither limited by the amplifier chain nor the CBC interferometer. Therefore, it would be probably possible to use the seed source and its actuators to actively stabilize the frequency. This particular approach has been used to reach frequency stability levels required by GWDs [28].

Furthermore, the two actuator signals and the in-loop error signal were monitored to evaluate the CBC interferometer and the phase control loop. The free-running differential phase noise was calculated using these monitored signals and is shown in Fig. 8. It can be seen that the fiber stretcher is primarily stabilizing low frequency phase variation up to approximately 25 Hz, while the piezo mounted mirror stabilizes variations up to unity gain. As the interferometer arms were not balanced, the NPRO frequency noise couples to differential phase noise. The arm length imbalance is mainly created by the 40 m of optical fiber located within the stretcher and not by amplifier fiber length variations, which were below 0.1 m. The magnitude of this coupling was calculated considering an imbalance of 40 m and by projecting the seed laser's frequency noise to the interferometer's differential phase noise. It can be seen, that the frequency noise of the seed laser did not significantly contribute to the overall free running differential phase noise.

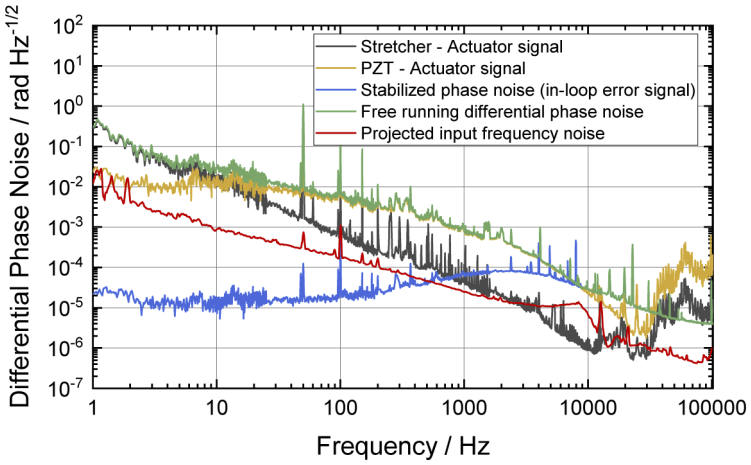

Fig. 8. Differential phase noise of the two amplifiers as free running and stabilized noise. The projected seed frequency noise is plotted as reference.

4. Conclusion

Power scaling of lasers with kilohertz linewidth at a wavelength of 1064 nm up to the 400 W level was demonstrated by filled-aperture coherent beam combination of two fiber amplifier chains. The combined beam was analyzed according to the application requirements of gravitational wave detection. This includes the measurement of the TEM_{00}-mode content, relative power noise, relative pointing noise, and frequency noise. Furthermore, the phase control loop was characterized and the differential phase noise between the two interferometer arms was evaluated. It was shown that the low noise performance of the single amplifier beams was mainly preserved. An optical power of 370 W in a linear polarized TEM_{00}-mode with low noise properties for the use in GWDs was demonstrated. This marks, to our knowledge, the highest reported optical power in the TEM_{00}-mode with these low noise beam properties.

Funding. Deutsche Forschungsgemeinschaft (EXC2123 QuantumFrontiers 390837967).

Optics EXPRESS

Acknowledgments. We would like to thank Thomas Theeg from FiberBridge Photonics GmbH for the ongoing and successful cooperation in the field of fiber component technology. Partially funded by the Deutsche Forschungsgemeinschaft (DFG, German Research Foundation) under Germany's Excellence Strategy EXC2123 QuantumFrontiers 390837967.

Disclosures. The authors declare no conflicts of interest.

References

1. B. P. Abbott, R. Abbott, T. D. Abbott, M. R. Abernathy, F. Acernese, and K. Ackley, *et al.*, "Observation of gravitational waves from a binary black hole merger," Phys. Rev. Lett. **116**(6), 061102 (2016).
2. B. P. Abbott, R. Abbott, T. D. Abbott, F. Acernese, K. Ackley, and C. Adams, *et al.*, "GW170817: Observation of gravitational waves from a binary neutron star inspiral," Phys. Rev. Lett. **119**(16), 161101 (2017).
3. B. P. Abbott, R. Abbott, T. D. Abbott, M. R. Abernathy, K. Ackley, and C. Adams, *et al.*, "Exploring the Sensitivity of Next Generation Gravitational Wave Detectors," Classical Quantum Gravity **34**(4), 044001 (2017).
4. M. Punturo, M. Abernathy, F. Acernese, B. Allen, N. Andersson, and K. Arun, *et al.*, "The third generation of gravitational wave observatories and their science reach," Classical Quantum Gravity **27**(8), 084007 (2010).
5. K. Ackley, V. B. Adya, P. Agrawal, P. Altin, G. Ashton, and M. Bailes, *et al.*, "Neutron star extreme matter observatory: A kilohertz-band gravitational-wave detector in the global network," Publ. Astron. Soc. Aust. **37**, e047 (2020).
6. C. Darsow-Fromm, M. Schröder, J. Gurs, R. Schnabel, and S. Steinlechner, "Highly efficient generation of coherent light at 2128?nm via degenerate optical-parametric oscillation," Opt. Lett. **45**(22), 6194–6197 (2020).
7. F. Thies, N. Bode, P. Oppermann, M. Frede, B. Schulz, and B. Willke, "Nd:YVO_4 high-power master oscillator power amplifier laser system for second-generation gravitational wave detectors," Opt. Lett. **44**(3), 719–722 (2019).
8. L. Winkelmann, O. Puncken, R. Kluzik, C. Veltkamp, P. Kwee, J. Poeld, C. Bogan, B. Willke, M. Frede, J. Neumann, P. Wessels, and D. Kracht, "Injection-locked single-frequency laser with an output power of 220 W," Appl. Phys. B: Lasers Opt. **102**(3), 529–538 (2011).
9. N. Bode, F. Meylahn, and B. Willke, "Sequential high power laser amplifiers for gravitational wave detection," Opt. Express **28**(20), 29469–29478 (2020).
10. M. Steinke, H. Tünnermann, V. Kuhn, T. Theeg, M. Karow, O. de Varona, P. Jahn, P. Booker, J. Neumann, P. Wßels, and D. Kracht, "Single-frequency fiber amplifiers for next-generation gravitational wave detectors," IEEE J. Sel. Top. Quantum Electron. **24**(3), 1–13 (2018).
11. E. Peral and A. Yariv, "Degradation of modulation and noise characteristics of semiconductor lasers after propagation in optical fiber due to a phase shift induced by stimulated Brillouin scattering," IEEE J. Quantum Electron. **35**(8), 1185–1195 (1999).
12. M. Karow, C. Basu, D. Kracht, J. Neumann, and P. Weßels, "TEM_{00} mode content of a two stage single-frequency Yb-doped PCF MOPA with 246 W of output power," Opt. Express **20**(5), 5319–5324 (2012).
13. J. Zhao, G. Guiraud, C. Pierre, F. Floissat, A. Casanova, A. Hreibi, W. Chaibi, N. Traynor, J. Boullet, and G. Santarelli, "High-power all-fiber ultra-low noise laser," Appl. Phys. B: Lasers Opt. **124**(6), 114 (2018).
14. C. Robin, I. Dajani, and B. Pulford, "Modal instability-suppressing, single-frequency photonic crystal fiber amplifier with 811 W output power," Opt. Lett. **39**(3), 666–669 (2014).
15. S. Hochheim, M. Steinke, P. Wessels, O. de Varona, J. Koponen, T. Lowder, S. Novotny, J. Neumann, and D. Kracht, "Single-frequency chirally coupled-core all-fiber amplifier with 100 W in a linearly polarized TEM_{00} mode," Opt. Lett. **45**(4), 939–942 (2020).
16. C. Dixneuf, G. Guiraud, Y.-V. Bardin, Q. Rosa, M. Goeppner, A. Hilico, C. Pierre, J. Boullet, N. Traynor, and G. Santarelli, "Ultra-low intensity noise, all fiber 365 W linearly polarized single frequency laser at 1064 nm," Opt. Express **28**(8), 10960–10969 (2020).
17. H. Tünnermann, J. H. Pöld, J. Neumann, D. Kracht, B. Willke, and P. Weßels, "Beam quality and noise properties of coherently combined ytterbium doped single frequency fiber amplifiers," Opt. Express **19**(20), 19600–19606 (2011).
18. L.-W. Wei, F. Cleva, and C. N. Man, "Coherently combined master oscillator fiber power amplifiers for Advanced Virgo," Opt. Lett. **41**(24), 5817–5820 (2016).
19. S. J. Augst, T. Y. Fan, and A. Sanchez, "Coherent beam combining and phase noise measurements of ytterbium fiber amplifiers," Opt. Lett. **29**(5), 474–476 (2004).
20. C. X. Yu, S. J. Augst, S. M. Redmond, K. C. Goldizen, D. V. Murphy, A. Sanchez, and T. Y. Fan, "Coherent combining of a 4 kW, eight-element fiber amplifier array," Opt. Lett. **36**(14), 2686–2688 (2011).
21. A. Flores, T. M. Shay, C. A. Lu, C. Robin, B. Pulford, A. D. Sanchez, D. W. Hult, and K. B. Rowland, "Coherent beam combining of fiber amplifiers in a kW regime," in *CLEO:2011 - Laser Applications to Photonic Applications*, (Optical Society of America, 2011), p. CFE3.
22. F. Wellmann, M. Steinke, F. Meylahn, N. Bode, B. Willke, L. Overmeyer, J. Neumann, and D. Kracht, "High power, single-frequency, monolithic fiber amplifier for the next generation of gravitational wave detectors," Opt. Express **27**(20), 28523–28533 (2019).
23. F. Wellmann, M. Steinke, P. Wessels, N. Bode, F. Meylahn, B. Willke, L. Overmeyer, J. Neumann, and D. Kracht, "Performance study of a high-power single-frequency fiber amplifier architecture for gravitational wave detectors," Appl. Opt. **59**(26), 7945–7950 (2020).
24. P. Kwee, F. Seifert, B. Willke, and K. Danzmann, "Laser beam quality and pointing measurement with an optical resonator," Rev. Sci. Instrum. **78**(7), 073103 (2007).

Optics EXPRESS

25. A. Klenke, S. Breitkopf, M. Kienel, T. Gottschall, T. Eidam, S. Hädrich, J. Rothhardt, J. Limpert, and A. Tünnermann, "530 W, 1.3 mJ, four-channel coherently combined femtosecond fiber chirped-pulse amplification system," Opt. Lett. **38**(13), 2283–2285 (2013).
26. H. Tünnermann, J. Neumann, D. Kracht, and P. Weßels, "Gain dynamics and refractive index changes in fiber amplifiers: a frequency domain approach," Opt. Express **20**(12), 13539–13550 (2012).
27. A. Buikema, C. Cahillane, G. L. Mansell, C. D. Blair, R. Abbott, and C. Adams, *et al.*, "Sensitivity and performance of the advanced ligo detectors in the third observing run," Phys. Rev. D **102**(6), 062003 (2020).
28. P. Kwee, C. Bogan, K. Danzmann, M. Frede, H. Kim, P. King, J. Pöld, O. Puncken, R. L. Savage, F. Seifert, P. Wessels, L. Winkelmann, and B. Willke, "Stabilized high-power laser system for the gravitational wave detector advanced LIGO," Opt. Express **20**(10), 10617–10634 (2012).
29. M. Tröbs, P. Weßels, and C. Fallnich, "Power- and frequency-noise characteristics of an Yb-doped fiber amplifier and actuators for stabilization," Opt. Express **13**(6), 2224–2235 (2005).